JOURNAL OF SOLID STATE CHEMISTRY 96, 287–293 (1992)

Synthesis, Structural Investigation, and Physical Characterization of Chromium Fluoride/Graphite Intercalation Compounds

K. AMINE, A. TRESSAUD, H. IMOTO,* J. GRANNEC, AND J. M. DANCE

Laboratoire de Chimie du Solide du CNRS, Université de Bordeaux I, 351, cours de la Libération, 33405 Talence Cedex, France

AND C. HAUW

Laboratoire de Cristallographie et de Physique Cristalline, Université de Bordeaux I, 33405 Talence Cedex, France

Received January 2, 1991; in revised form July 15, 1991

Intercalation into graphite of CrF_4 containing some amounts of CrF_5 has been investigated using anhydrous HF solutions. Stage-2 GICs are generally obtained with repeat distance $I_c = 11.45$ Å, whatever the pristine graphite material. The I_c value corresponds to CrF_6 octahedra with two faces lying parallel to the graphene layers. The fitting of the intensities of the (00*l*) powder diffraction lines and the relationships between the unit cells of the graphite and of the intercalate sublattices leads to a theoretical $C_{18}CrF_{4.5}$ formulation which is in good agreement with the observed composition, i.e., $C_xCrF_{4.5}$ with $17 \lesssim x \lesssim 21$. XANES. ESR, and magnetic measurements have confirmed the (+IV) oxidation state of the intercalated chromium and have corroborated the charge transfer evaluation from reflectivity data.

I. Introduction

The range of oxidation states known for chromium fluorides is the largest among the 3*d*-transition metal fluorides, since it includes every state from (+II) in CrF_2 to (+VI) in CrF_6. As in the other series of *d*-transition metals, the melting temperatures of binary fluorides are known to decrease with increasing oxidation state, at least for the higher states. Whereas CrF_2 and CrF_3 melt above 800°C, CrF_4 sublimes in vacuum at about 100°C and CrF_5 melts at 30°C; CrF_6 is thermally unstable above −100°C (*1*).

Although many transition metal fluorides have been inserted in graphite, the only intercalated chromium-based species was CrO_2F_2 (*2–4*). Since CrF_4 seemed to be a good candidate for such a purpose, the intercalation process of this material in graphite has been investigated. The present work is focused on the synthesis and on the physical characterization of chromium fluoride GICs (Graphite Intercalation Compound) obtained using anhydrous HF (AHF) medium. The optical determination of the charge transfer in this material has been published elsewhere (*5*).

II. Experimental

1. Starting Materials

CrF_4 was prepared by direct fluorination of CrF_3. Chromium trifluoride was treated

* Permanent address: Sony Corp. Research Center, Hodogaya-ku, Yokohama 240, Japan.

0022-4596/92 $3.00

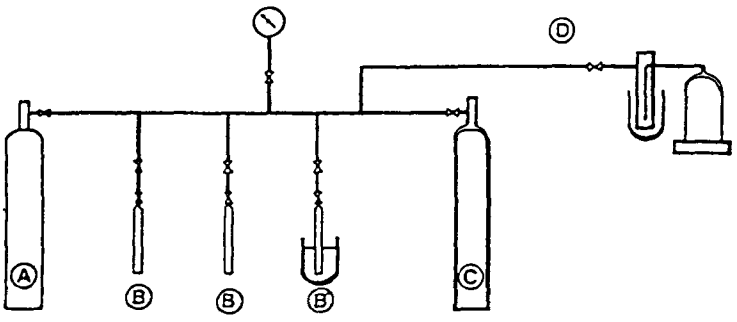

FIG. 1. Schematized set up for the intercalation process in AHF: Ar cylinder (A); FEP tubes (B); HF cylinder (C); vacuum pump and line (D).

under 2 bar of pure fluorine gas for 6 hr at 350°C in a passivated nickel reactor. After it cooled down to room temperature, the container was refilled with fluorine gas, and the treatment cycle was repeated in order to bring the reaction to completion. It should be noted that the fluorination process yields some CrF_5 as a side product (*1, 6, 7*). The pentafluoride, which is more volatile than CrF_4, was mainly condensed on the cooled upper part of the container, but also unavoidably mixed to some extent with CrF_4, less than 5% in any case.

2. *Intercalation Process in AHF*

The intercalation of CrF_4, containing therefore small amounts of CrF_5, was carried out in AHF at room temperature. The experimental set up is schematized in Fig. 1. The different tubes connected to the metal line were made of a transparent polymer, fluoroethylenepropylene (FEP), which is completely inert with respect to HF and to other fluorine-based reagents. HF was condensed from cylinder C into one of the tubes B using liquid nitrogen as coolant. This tube contained powdered BiF_5 or another perfluorinated inorganic species such as $M_2Ni^{IV}F_6$, $M_3Cu^{III}F_6$ (M = alkali element). This step was essential for two purposes: (i) purification of the solution by trapping all traces of moisture, and (ii) saturation of the AHF solution with fluorine produced, for instance, during the dissociation of some amounts of the perfluorinated species.

HF was then transferred in the same way to another tube B, which had been previously filled in a dry atmosphere with a mixture of host graphite sample and of chromium fluoride to be intercalated. A slight outgassing of the solid was immediately observed. This phenomenon, which results probably from a reduction of CrF_5, could be responsible for the triggering of the insertion mechanism by preliminary oxidation of the graphite, following the reaction

$$C_x + \tfrac{1}{2}F_2 + CrF_y^- + H_2F^+ \rightarrow C_x^{\delta+}CrF_y^{\delta-} + 2HF.$$

Such a mechanism has already been proposed for the insertion of SnF_4 into graphite (*8*).

After the reaction, the blue colored GICs were stable in humid air. They were washed in ethanol or in diluted HCl in order to eliminate traces of noninserted metal fluorides deposited onto the sample surface.

3. *Chemical and Physical Characterizations*

The composition of GICs were determined from electron microprobe analyses using standard samples containing the same components in appropriate amounts. The

elemental analyses were carried out at CNRS-Service Central d'Analyse : carbon was analyzed by infrared or coulometric detection of CO_2 produced by high temperature combustion of the sample, chromium was titrated using absorption spectrometry, and fluorine thanks to a specific electrode.

Powder diffraction techniques were used to determine the stage number, the repeat distance I_c along c-axis, and the intercalate thickness. The diffraction spectra were recorded on a Philips diffractometer using filtered CuK_α radiation. The spatial distribution of the intercalated species was determined by precession photographs taken at room temperature using MoK_α radiation.

Magnetic measurements were performed on a SQUID magnetometer in the 2–300 K temperature range under an applied field of 0.5 T. ESR spectra were obtained on a Bruker E.R. 200 tt spectrometer working in the X-band in a TE 102 mode cavity. The applied magnetic field could range from 0 to 0.8 T, with a modulation frequency of 100 kHz.

XANES (X-ray Absorption Near Edge Structure) was used to determine the oxidation state of the intercalated metal. These experiments were carried out at LURE (Université de Paris-Sud, Orsay), using DCI synchroton radiation.

III. Structural Properties

A typical diffraction pattern of a chromium fluoride GIC is shown in Fig. 2(a). Whatever the starting graphite material, i.e., either HOPG, flaky natural graphite (NG), or highly purified natural powder graphite (SP1 grade, $\emptyset \approx 30\ \mu$m, Union Carbide Co.), the final GICs are stage-2 compounds with a repeat distance $I_c = 11.45$ Å and an intercalate thickness $d_i = 4.75$ Å. The latter value corresponds to the distance between two parallel faces of a CrF_6 octahedron containing Cr(+IV) : $d = 4.83$ Å, rather than Cr(+III) : $d = 4.90$ Å (*9*). These results would suggest that the environment of chromium has been preserved during the intercalation.

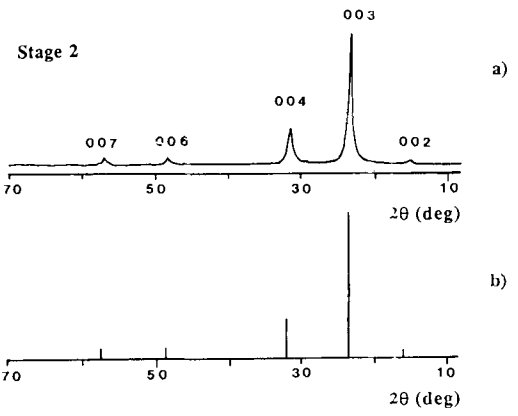

FIG. 2. Experimental XRD pattern of a stage-2 C_xCrF_y compound (a), compared with a calculated one with $x = 18$ and $y = 4.5$ (b).

Theoretical intensities of (00l) reflections have been, therefore, calculated for the assumption of intercalated MF_6 octahedra with two faces parallel to the graphene layers. The intensity of the (00l) diffraction peaks is related to the structure factor F by the relation

$$I_{(00l)} = [F_{(00l)}]^2 \times LP,$$

in which LP represents the Lorentz-polarization factor: $LP = (1 + \cos^2 2\theta)/\sin 2\theta$ for two-dimensional structures such as graphite and GICs. If the chromium layer is chosen as the origin, the structure factor for a GIC compound with a C_xCrF_y formula can be written

$$F_{001} = [f_{Cr^{4+}} + yf_{F^-} \cos 2\pi l z_1 + xf_C \cos 2\pi l z_2] \exp(-B \sin^2\theta)/\lambda^2,$$

where f are the atomic diffusion factors, l the position in the reciprocal space, z_1 = Cr–F and z_2 = Cr–C are distances along the c-axis. As only 11 reflections were available, the B factor has been fixed to 4 Å^2. The best

TABLE I

COMPARISON OF THE OBSERVED (00*l*) INTENSITIES OF STAGE-2 C_xCrF_y COMPOUNDS WITH CALCULATED ONES WITH $x = 18$ AND $y = 4.5$

d(Å)	l	LP	$I_{obs.}$	$I_{calc.}$
11.458	1	14.75	2.6	3.9
5.729	2	7.23	4.2	4.1
3.819	3	4.66	100	100
2.865	4	3.66	27.5	25.8
2.292	5	2.522	0	0.1
1.910	6	1.968	2.3	1.8
1.637	7	1.576	3.1	2.7
1.432	8	1.297	1.1	0.7
1.273	9	1.11	0.9	0.6
1.146	10	1.013	0	0.1
1.042	11	1.012	1.0	0.6

agreement between the simulated pattern and the experimental one is obtained for $x = 18$ and $y = 4.5$, i.e. for a composition $C_{18}CrF_{4.5}$. A comparison of the observed (001) intensities and calculated ones is given in Table I and Fig. 2.

This result is in fairly good agreement with the experimental compositions as deduced by two different ways: an approximate composition $C_{17\pm2}Cr_{1\pm0.1}F_{4.7\pm0.2}$ has been obtained from electron microprobe analysis on NG-based GICs, whereas elemental analysis on HOPG-based GICs yielded $C_{21\pm2}Cr_{1\pm0.1}F_{4.5\pm0.2}$.

In order to obtain additional information concerning the organization and orientation of the intercalated species with respect to the graphite network, precession photographs have been realized on selected NG crystals as shown in Fig. 3. Besides intense spots corresponding to the graphite hexagonal network, weaker spots belong to the intercalated fluoride species and can be attributed to a hexagonal lattice with a 7.38 Å edge. Its orientation with respect to the graphite axes is 40°. This sublattice exhibits three equivalent orientations related to each other by a 60° rotation. The ratio of the parameter of the intercalated fluoride cell ($a_{int.} = 7.38$ Å) to that of graphite ($a_{gr.} = 2.46$ Å) is an integer: $a_{int.}/a_{gr.} = 3$. The intercalate sublattice could be considered as commensurate to that of graphite provided a 40° rotation. The area of the intercalate unit cell is 18 times larger than that occupied by a carbon atom. In addition, as the GICs are stage-2, the intercalated layers are separated from each other by two carbon planes. Therefore, the intercalate cell corresponds to $18 \times 2 = 36$ C atoms. By taking the atomic ratio F/Cr = 4.5 as obtained from the chemical analyses, a calculated composition of $C_{36}Cr_2F_9$—i.e., $C_{18}CrF_{4.5}$, which is a formula close to the experimental one—is reached if we consider the presence of two Cr atoms only in the intercalate cell. This compound is therefore characterized by an incomplete filling of the interlayer space, as are most of metal halide GICs.

In conclusion, both simulation of the powder diffractograms and calculation based on geometrical relationships between the graphite and the intercalate sublattices lead to compositions in reasonable agreement with the analyses.

IV. Determination of the Oxidation State of Intercalated Chromium

1. Magnetic Investigation

The temperature dependence of the reciprocal magnetic susceptibility of a stage-2 HOPG-based GIC of composition $C_{21}CrF_{4.5}$ is shown in Fig. 4. The susceptibility obeys a Curie–Weiss law with $\theta_p = -13$ K. The value of the Curie constant, $C = 0.95$ emu K mol^{-1}, corresponds to an effective moment $\mu_{eff.} = 2.76$ BM using the $C = \mu_{eff}^2/8$ formula. From the comparison of the experimental moment with those calculated for different chromium oxidation states, it appears that the transition metal is mostly inserted in its tetravalent state (Cr^{4+}: $^3F_2$ spectral term; $S = 1$, $\mu_{eff.}$ calculated with a quenched orbital moment: 2.82 BM). This result has been confirmed by an optical reflectivity

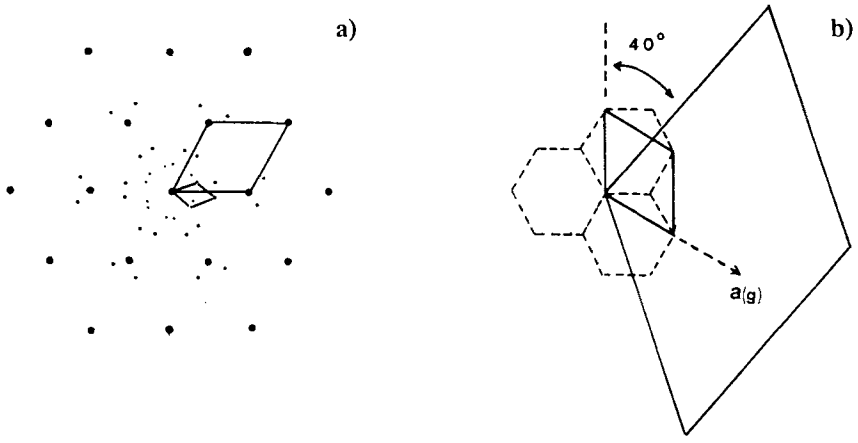

FIG. 3. NG-based C_xCrF_y crystal: schematized lattice showing graphite and intercalate unit cells in the reciprocal space (a); relationships between graphite and intercalate unit cells in the direct space (b).

study which has shown that the charge transfer between the intercalated species and graphite is about 0.5 e^-. The GIC formula could be therefore written $C_{21}^{0.5+}$ $(CrF_{4.5})^{0.5-}$ (*5*).

No tridimensional magnetic ordering has been found down to 2 K, contrary to $NiCl_2$- or $CoCl_2$-based GICs. The absence of a transition can be explained by the large distance separating two intercalate layers in the stage-2 network, i.e., 11.45 Å, and by the small number of unpaired electrons present in Cr(+IV)(d^2).

2. *XANES Study*

An X-ray absorption spectrum can be divided into two parts: the first one, which is situated at energies near the absorption threshold, corresponds to XANES; the second one, situated at higher energies, refers to the EXAFS domain (Extended X-ray Absorption Fine Structure) (*10*). In the first

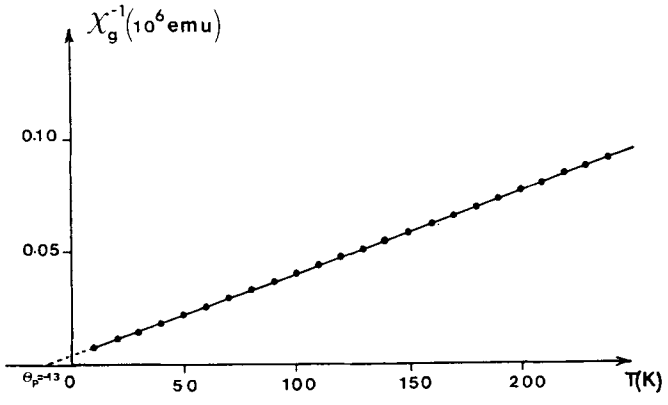

FIG. 4. Temperature dependence of the reciprocal magnetic susceptibility of $C_{21}CrF_{4.5}$.

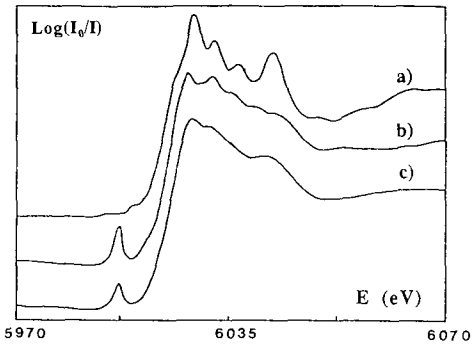

FIG. 5. X-ray absorption spectra at Cr *K*-edge of several chromium fluorocompounds: CrF_3 (a); Na_2CrF_6 (b); $C_{21}CrF_{4.5}$ (c).

part, the position and the envelope of the spectrum depend on different physical parameters, such as site symmetry, formal and effective charge of the absorbing atom (*11*).

We have therefore compared the signal of the chromium fluoride-GIC with those of CrF_3 and Na_2CrF_6 in which chromium exhibits, respectively, (+III) and (+IV) oxidation states for the same type of environment, i.e., for CrF_6 octahedra. Figure 5 shows XANES absorption spectra of these compounds at Cr *K*-edge in the 5970–6070 eV energy range with an energy resolution of 0.2 eV. The experimental envelopes are similar to those obtained from multiple scattering calculation for CrO_6 units (*12*).

The spectrum of CrF_3 is characterized by the absence of a peak in the prethreshold region; on the other hand, the spectra of Na_2CrF_6 and $C_xCrF_{4.5}$ present a prethreshold peak at the same energy: $E = 5994$ eV. This peak, which corresponds to a $1s \rightarrow 3d$ quadrupolar transition, is enhanced for increasing oxidation states because of the higher number of *d* empty orbitals (*11*). The XANES data seem to confirm, therefore, that in $C_xCrF_{4.5}$ the actual oxidation state of intercalated chromium is (+IV).

An EXAFS study is in progress to determine the environment of chromium in this type of materials, but preliminary results seem to show that the first coordination shell is noticeably distorted.

3. *ESR Investigation*

The experimental ESR spectrum of NG-based chromium fluoride-GIC is shown in Fig. 6. The anisotropy of the signal can be related to the anisotropy of the electronic configuration of intercalated chromium associated with an axial distortion of the CrF_6 octahedra; *g*-values have been deduced from computer simulations. Although a finite value is assigned for $g_\perp$, a fluctuation of the $g_{/\!/}$ values is necessary to obtain a good fitting of the spectrum. The best agreement is obtained for $g_\perp = 1.978$ and $g_{/\!/} = 1.895 \pm 0.015$ (Fig. 6). This fluctuation could refer to a combination of different Cr–F distances in the direction of the axial distortion.

The hypothesis of the presence of a distorted chromium fluoride species is consistent with a previous ESR study of Al_2O_3 doped by tetravalent chromium (*13*). In these experiments, the excess of positive charges was compensated by substitution of nitrogen for oxygen. The authors observed an anisotropic signal identical to that of C_xCrF_y, with almost the same *g*-values ($g_\perp = 1.98$; $g_{/\!/} = 1.90$), and they showed that chromium occupied a distorted octahedral environment. Another possibility for

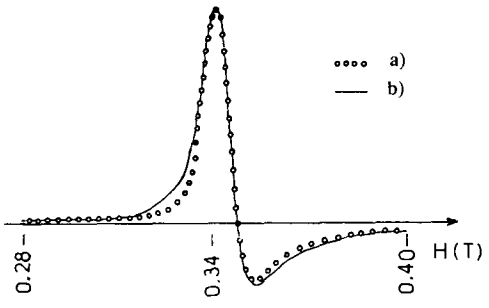

FIG. 6. ESR spectra of a NG-based $C_xCrF_{4.5}$ compound: experimental ($\nu = 9.46$ GHz) (a); simulated with *g*-values given in the text (b).

the origin of the ESR signal would have been the conduction ESR spectrum with a Dysonian lineshape, as observed in others GICs (14, 15). However, in these cases the g-values are very close to the free electron one, and the linewidth is somewhat smaller.

V. Conclusions

Among chromium fluorides and oxyfluorides, only CrO_2F_2 had been so far intercalated in graphite from $K_2Cr_2O_7$ solutions in AHF (*2–4*). The thickness of the intercalate $d_i = 4.60$ Å could be deduced from the repeat distance ($I_c = 7.95$ Å) of the obtained stage-1 compound. An octahedral coordination had been proposed for pure CrO_2F_2 (*16*), as observed in all known chromium fluorides and oxyfluorides. The larger intercalate thickness that has been observed in $C_xCrF_{4.5}$ ($d_i = 4.75$ Å) is in good agreement with a (+IV) oxidation state, when compared with (+VI) oxidation state in $C_xCrO_2F_2$.

The intercalation into graphite of CrF_4 containing small amounts of CrF_5 using AHF solutions is followed by a charge coefficient $f = 0.50$ per intercalated species (*5*). The (+IV) oxidation state of the inserted chromium has been proposed to explain this value and fits with the experimental composition $C_xCrF_{4.5\pm0.2}$ (with $17 \lesssim x \lesssim 21$); this result has been confirmed using several physical measurement techniques, including magnetic measurements, XANES, and ESR. In addition, the observed nominal composition of the material accounts for the calculated (001) intensities of the X-ray diffraction powder pattern and for the dimensions of the intercalated sublattice.

Acknowledgments

The authors are indebted to Prof. P. Hagenmuller, T. Nakajima (Kyoto University), H. Dexpert (LURE), T. Roisnel (L.L.B. Saclay), and E. Fargin for valuable discussions.

References

1. R. Colton and J. H. Canterford, "Halides of the First Row Transition Metals," Wiley–Interscience, London (1969).
2. E. Buscarlet, Thesis, Univ. Grenoble, France (1976).
3. A. Hamwi, P. Touzain, and L. Bonnetain, *Rev. Chim. Miner.* **19,** 651 (1982).
4. H. Selig, *J. Fluorine Chem.* **45,** 72 (1989).
5. K. Amine, A. Tressaud, P. Hagenmuller, H. Imoto, H. Touhara, and T. Nakajima, *Mater. Res. Bull.*, **25,** 1219 (1990).
6. E. G. Hope, P. J. Janes, W. Levason, J. S. Ogden, M. Tajik, and J. W. Turff, *J. Chem. Soc., Dalton Trans.*, 1443 (1985).
7. H. C. Clark and Y. N. Sadana, *Can. J. Chem.* **42,** 50 (1964).
8. K. Kadono, Ph. D. Thesis, Kyoto Univ., Japan (1986).
9. Ionic radii have been taken from R. D. Shannon, *Acta Crystallogr., Sect. A: Cryst. Phys., Diffr. Theor. Gen. Crystallogr.* **A32,** 751 (1976).
10. H. P. Hanson and J. R. Knight, *Phys. Rev.* **102,** 632 (1956).
11. C. Cartier and M. Verdaguer, *J. Chim. Phys.* **86,** (7/8) (1989).
12. J. Garcia, A. Bianconi, M. Benfatto, and C. R. Natoli, *J. Phys.* **47**(12), 49 (1986).
13. R. H. Hoskins and B. H. Soffer, *Phys. Rev.* **33,** A490 (1964).
14. G. Ceotto, G. E. Barberis, and C. Rettori, *Synth. Met.* **34,** 557 (1989).
15. P. Lauginie, H. Estrade, B. Brousseau, and J. Conard, *Synth. Met.* **34,** 563 (1989).
16. A. J. Edwards and P. Taylor, *J. Chem. Soc. Chem. Commun.*, 1474 (1970).